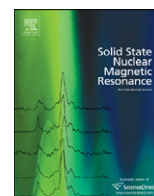




ELSEVIER

Contents lists available at SciVerse ScienceDirect

Solid State Nuclear Magnetic Resonance

journal homepage: www.elsevier.com/locate/ssnmrNMR study of the $\text{LiMnPO}_4 \cdot \text{OH}$ and $\text{MPO}_4 \cdot \text{H}_2\text{O}$ ($\text{M}=\text{Mn}, \text{V}$) homeotypic phases and DFT calculationsA. Castets^{a,b}, D. Carlier^{a,b,*}, Y. Zhang^c, F. Boucher^c, N. Marx^{a,b}, R. Gautier^d, E. Le Fur^d, L. Le Pollès^d, L. Croguennec^{a,b}, M. Ménétrier^a^a CNRS, Université de Bordeaux, ICMCB, 87 Avenue du Dr. A. Schweitzer, 33608 Pessac Cedex, France^b CNRS, ENSCBP, ICMCB, 87 Avenue du Dr. A. Schweitzer, 33608 Pessac Cedex, France^c Institut des Matériaux Jean Rouxel (IMN), Université de Nantes, CNRS, 2 rue de la Houssinière, BP 32229, 44322 Nantes Cedex, France^d CNRS, ENSCR, Avenue du Général Leclerc, CS50837, 35708 Rennes Cedex 7, France

ARTICLE INFO

Article history:

Received 18 July 2011

Received in revised form

20 October 2011

Available online 22 November 2011

Keywords:

Lithium battery electrodes

Fermi contact

MAS NMR

DFT calculations

GGA+U

Tavorite

ABSTRACT

Following our previous work on the tavorite-like $\text{LiFePO}_4 \cdot \text{OH}$ and $\text{FePO}_4 \cdot \text{H}_2\text{O}$ phases, we report here the magnetic and NMR characterizations of analogous $\text{LiMnPO}_4 \cdot \text{OH}$, $\text{MnPO}_4 \cdot \text{H}_2\text{O}$ and $\text{VPO}_4 \cdot \text{H}_2\text{O}$ phases together with the DFT calculations of the NMR shifts. The first two compounds exhibit Curie–Weiss type magnetic behavior with Curie constants close to the theoretical ones for HS Mn^{3+} , while the vanadium compound is very close to a pure Curie-type behavior. ^7Li , ^{31}P and ^1H MAS NMR spectra are reported for the three compounds, and show strong Fermi-contact shifts for the first two nuclei, while the sign and magnitude of the ^1H shifts are very different for the three phases.

DFT calculations (FLAPW in GGA+U approximation) using the WIEN2k code and the experimental susceptibilities are shown to reproduce closely the experimental data. This situation is compared to the case of the homologous and isostructural Fe compounds, which exhibit much more complex magnetic behaviors.

© 2011 Elsevier Inc. All rights reserved.

1. Introduction

In the context of our work on NMR in paramagnetic battery-related materials, we recently took interest in the NMR study (^7Li , ^{31}P and ^1H MAS NMR) and in the magnetic properties for the two compounds $\text{LiFePO}_4 \cdot \text{OH}$ (tavorite) and $\text{FePO}_4 \cdot \text{H}_2\text{O}$, potential candidates for electrode materials in Li-ion batteries, and suitable materials for investigating the calculation strategies of the NMR (contact) shifts in paramagnetic compounds (high spin Fe^{3+} in both phases), a topic presently investigated by several research groups [1–3]. Taking into account the experimental magnetic susceptibility at the temperature of the NMR measurement and using the electron spin density at the nucleus obtained from FLAPW-type calculations led to rather satisfactory agreement between calculated NMR shifts and experimental ones of ^7Li , ^{31}P and ^1H for $\text{LiFePO}_4 \cdot \text{OH}$ and $\text{FePO}_4 \cdot \text{H}_2\text{O}$. However, GGA+U approximation is more appropriated for the former compound while GGA appears more suitable for the later one.

In order to analyze the relevance of such strategies, they indeed need to be applied to a broader range of materials. Since

the $\text{LiMPO}_4 \cdot \text{OH}$ – $\text{MPO}_4 \cdot \text{H}_2\text{O}$ family extends to other transition metals, and therefore other electronic configurations, we extend our work in the same spirit as for the Fe phases.

In the present paper, we focus on the $\text{LiMnPO}_4 \cdot \text{OH}$, $\text{MnPO}_4 \cdot \text{H}_2\text{O}$ and $\text{VPO}_4 \cdot \text{H}_2\text{O}$ phases. The structures of $\text{LiFePO}_4 \cdot \text{OH}$ and $\text{FePO}_4 \cdot \text{H}_2\text{O}$ are presented in Fig. 1 [4,5], as representative of those of the Mn and V phases. All these structures are homeotypic, and formed by chains of MO_6 ($\text{M}=\text{Fe}, \text{Mn}, \text{V}$) octahedra interconnected by PO_4 tetrahedra, thus forming several types of tunnels. The difference between the $\text{LiFePO}_4 \cdot \text{OH}$ and $\text{FePO}_4 \cdot \text{H}_2\text{O}$ structures resides in the distortion of FeO_6 octahedra along the chains, those being responsible for a change in the unit cell symmetry described by a triclinic ($P-1$ $\text{LiFePO}_4 \cdot \text{OH}$) or a monoclinic ($C2/c$ $\text{FePO}_4 \cdot \text{H}_2\text{O}$) space group. In the case of the Fe phases, X-ray and neutron diffraction studies led to two positions for Fe in $\text{LiFePO}_4 \cdot \text{OH}$ whereas there is only one for $\text{FePO}_4 \cdot \text{H}_2\text{O}$ [4,5]. In $\text{LiFePO}_4 \cdot \text{OH}$, the Li atoms are located in the tunnels along the c axis and occupy a single site. In the two Fe phases, the P atoms occupy a single site. The H atoms in $\text{FePO}_4 \cdot \text{H}_2\text{O}$ and the one in $\text{LiFePO}_4 \cdot \text{OH}$ were shown to be bound to the oxygen atoms bridging two adjacent FeO_6 octahedra in the chains.

As mentioned, the $\text{LiMnPO}_4 \cdot \text{OH}$ and $\text{MPO}_4 \cdot \text{H}_2\text{O}$ ($\text{M}=\text{Mn}, \text{V}$) phases possess the same structures as the $\text{LiFePO}_4 \cdot \text{OH}$ and $\text{FePO}_4 \cdot \text{H}_2\text{O}$ ones, respectively, as described in the literature [6–13]. However, for the Mn and V phases, the hydrogens have not been localized to our best knowledge.

* Corresponding author at: CNRS, ENSCBP, ICMCB, 87 Avenue du Dr. A. Schweitzer, 33608 Pessac Cedex, France. Fax: +33 5 40 00 27 61.

E-mail address: carlier@icmcb-bordeaux.cnrs.fr (D. Carlier).

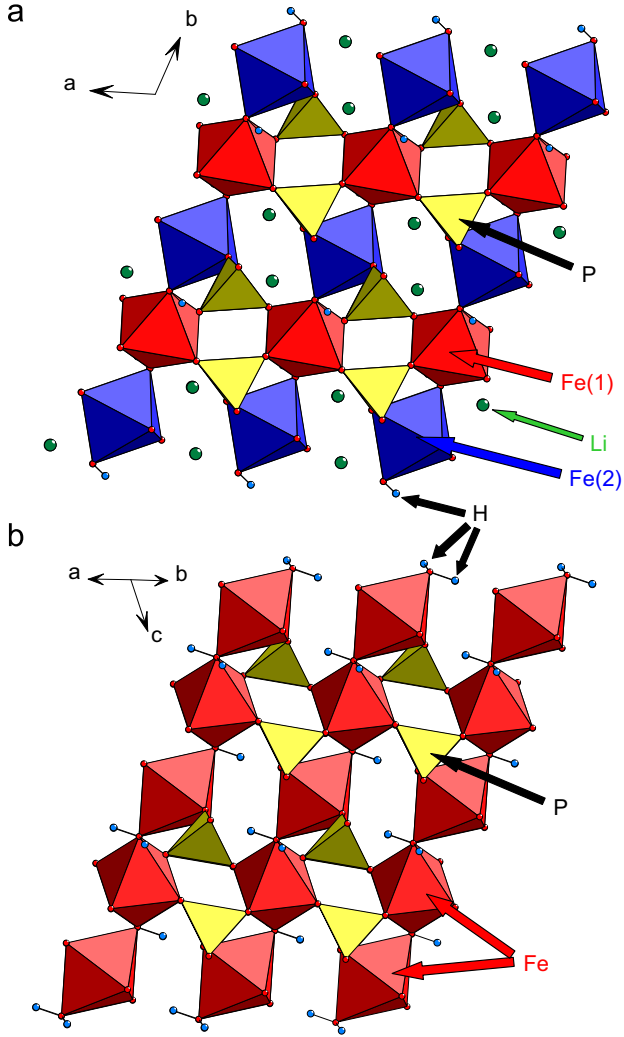


Fig. 1. Structure of (a) $\text{LiFePO}_4 \cdot \text{OH}$ (from Ref. [5]) and (b) $\text{FePO}_4 \cdot \text{H}_2\text{O}$ (from Ref. [4]).

All these paramagnetic compounds lead to NMR spectra dominated by interactions between nuclear and electron spins (hyperfine interactions). The Fermi contact shift, which governs the NMR signal of such compounds, corresponds to the presence of some density of electron spin at the nucleus probed. The sign and magnitude of the Fermi contact shift produced by this local magnetization for a given nucleus (i) can be expressed as follows [14], with the so-called contact coupling constant A^i :

$$\delta_{iso}^i = \frac{A^i}{h} \frac{\chi_M}{\mu_0 \gamma^i g_e \mu_B} \quad (1)$$

where χ_M is the magnetic susceptibility (related to one mole of transition metal), h is Planck's constant, μ_0 is the magnetic permeability, γ^i is the nuclear gyromagnetic ratio, g_e is the electron g factor and μ_B is the Bohr magneton.

As described in the literature, the coupling constant is proportional to the density of electron spin at the site of the nucleus (as being transferred in effect from the various paramagnetic ions in the surrounding of the atom considered) [15]:

$$A^i = \frac{\mu_0}{3S} h \gamma^i g_e \mu_B \rho^i(0) \quad (2)$$

where S is the spin quantum number of the paramagnetic ion and $\rho^i(0)$ is the spin density at or near the nucleus considered.

Therefore, the contact shift can be expressed as

$$\delta_{iso}^i = \frac{1}{3S} \rho^i(0) \chi_M \quad (3)$$

Modeling strategies enable the understanding of the electron spin transfer mechanisms based on delocalization or polarization-type mechanisms leading to positive or negative Fermi contact shifts, respectively [16]. This first approach based on plane wave/pseudo-potential calculations at 0 K with the VASP code can deal with rather large supercells. It allows (even if not quantitatively) the assignment of the different Li sites in a given compound based on the 0 K spin density found in an ionic sphere around Li [16–18]. Other calculation codes such as the “GIPAW package” of quantum Espresso recently proposed the use of PAW approach to provide the hyperfine coupling constant based on the spin density at the nucleus. From such data, Mali et al. took into account the temperature in the paramagnetic regime, assuming an ideal Curie behavior to calculate the finite temperature NMR Fermi contact shift [1]. In another recent work by Kim et al. on different phosphates, an all-electron LCAO code (Crystal06) with B3LYP hybrid exchange-correlation functional was used to calculate the spin density at the nucleus at 0 K. The authors assumed Curie–Weiss type behaviors for the materials, with experimental determination of the magnetic parameters (C , θ) for finite temperature shift calculation [2]. In their study, these authors report the difficulty to select an appropriate basis for their calculations.

In our work on the Fe phases, we first applied the pseudo-potential method earlier developed by some of us to estimate at 0 K electron spin densities at the nucleus sites. We then calculated more accurately these quantities using the full potential-LAPW code WIEN2k in the GGA or GGA+U approximation from which the finite temperature NMR shifts were obtained using the experimental magnetic susceptibility. Contrarily to an LCAO method, the Full Potential WIEN2k/LAPW method uses an adaptive basis set whose completeness can be easily evaluated, and provides an accurate description of the spin density at the nuclei of interest from which the hyperfine field (HFF) can be extracted.

In the present work, we apply the same strategy as for the Fe phases to $\text{LiMnPO}_4 \cdot \text{OH}$, $\text{MnPO}_4 \cdot \text{H}_2\text{O}$ and $\text{VPO}_4 \cdot \text{H}_2\text{O}$, i.e. magnetic and NMR characterizations, and a calculation methodology with the VASP and WIEN2k codes.

In a forthcoming paper, we will focus on understanding and describing the spin transfer mechanisms in the Fe, Mn and V phases.

2. Experimental section

$\text{MnPO}_4 \cdot \text{H}_2\text{O}$ was obtained as described by Aranda et al. [11,19]. The sample was prepared by slowly adding, at ambient temperature, H_3PO_4 (85%) to an aqueous suspension of manganese (II) carbonate hydrate with the molar ratio $\text{H}_3\text{PO}_4:\text{MnCO}_3$ of 3:1. After release of CO_2 , nitric acid was added and the reaction mixture was boiled to oxidize Mn (II) to Mn (III), which resulted in the evolution of NO_2 and the formation of a dark green precipitate after one hour. The product was filtered out and dried at 80 °C overnight.

$\text{LiMnPO}_4 \cdot \text{OH}$ was obtained from $\text{MnPO}_4 \cdot \text{H}_2\text{O}$ through an H^+/Li^+ exchange as described by Aranda et al. [20]. $\text{MnPO}_4 \cdot \text{H}_2\text{O}$ was milled with an excess ($\text{Li}^+/\text{Mn}^{3+} \sim 4$) of lithium nitrate LiNO_3 , and then the mixture was heated at 200 °C for 2 weeks. After water washing and filtration, the product was dried at 80 °C overnight.

$\text{VPO}_4 \cdot \text{H}_2\text{O}$ was prepared by hydrothermal treatment. In a typical synthesis a mixture of VCl_3 , H_3PO_4 (85%) and water (molar

Download English Version:

<https://daneshyari.com/en/article/5420524>

Download Persian Version:

<https://daneshyari.com/article/5420524>

[Daneshyari.com](https://daneshyari.com)